ACS Medicinal Chemistry Letters

Featured Letter

pubs.acs.org/acsmedchemlett

Targeting Metal-Aβ Aggregates with Bifunctional Radioligand [^{11}C]L2-b and a Fluorine-18 Analogue [^{18}F]FL2-b

Brian P. Cary,[†,#] Allen F. Brooks,[†,#] Maria V. Fawaz,[†] Xia Shao,[†] Timothy J. Desmond,[†] Garrett M. Carpenter,[†] Phillip Sherman,[†] Carole A. Quesada,[†] Roger L. Albin,[‡,§,∥] and Peter J. H. Scott*[,†,⊥]

[†]Division of Nuclear Medicine, Department of Radiology, The University of Michigan Medical School, Ann Arbor, Michigan 48109, United States

[‡]Geriatrics Research, Education, and Clinical Center, Veterans Affairs Ann Arbor Healthcare System, Ann Arbor, Michigan 48105, United States

[§]Department of Neurology, The University of Michigan Medical School, Ann Arbor, Michigan 48109, United States

[∥]Michigan Alzheimer Disease Center, The University of Michigan, Ann Arbor, Michigan 48105, United States

[⊥]The Interdepartmental Program in Medicinal Chemistry, The University of Michigan, Ann Arbor, Michigan 48109, United States

Supporting Information

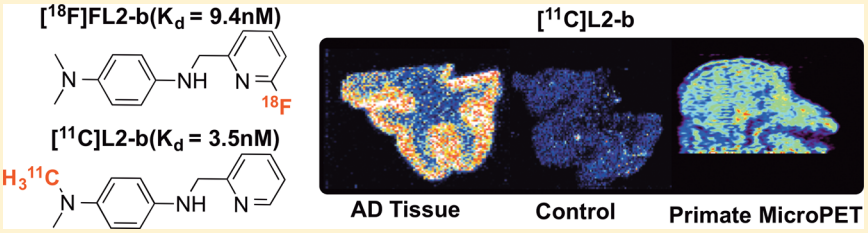

ABSTRACT: Interest in quantifying metal-Aβ species *in vivo* led to the synthesis and evaluation of [^{11}C]L2-b and [^{18}F]FL2-b as radiopharmaceuticals for studying the metallobiology of Alzheimer's disease (AD) using positron emission tomography (PET) imaging. [^{11}C]L2-b was synthesized in 3.6% radiochemical yield (nondecay corrected, n = 3), >95% radiochemical purity, from the corresponding desmethyl precursor. [^{18}F]FL2-b was synthesized in 1.0% radiochemical yield (nondecay corrected, n = 3), >99% radiochemical purity, from a 6-chloro pyridine precursor. Autoradiography experiments with AD positive and healthy control brain samples were used to determine the specificity of binding for the radioligands compared to [^{11}C]PiB, a known imaging agent for β-amyloid (Aβ) aggregates. The K_d for [^{11}C]L2-b and [^{18}F]FL2-b were found to be 3.5 and 9.4 nM, respectively, from those tissue studies. Displacement studies of [^{11}C]L2-b and [^{18}F]FL2-b with PiB and AV-45 determined that L2-b binds to Aβ aggregates differently from known radiopharmaceuticals. Finally, brain uptake of [^{11}C]L2-b was examined through microPET imaging in healthy rhesus macaque, which revealed a maximum uptake at 2.5 min (peak SUV = 2.0) followed by rapid egress (n = 2).

KEYWORDS: *Alzheimer's disease, amyloid-beta, metal ions, metal-Aβ, positron emission tomography, carbon-11, fluorine-18*

Alzheimer's disease (AD) is a neurodegenerative disorder with devastating socioeconomic costs and effects. With the aging of the population in the developed world, the number of cases of AD will increase.[1,2] While the need for better diagnostics and treatments are clear, the complexity of the pathogenesis of the disease represents a difficulty in achieving those goals. Radiopharmaceuticals for positron emission tomography (PET) imaging are a noninvasive means to detect AD onset, validate biomarkers, and monitor disease progression. There are presently several radiopharmaceuticals approved for use in the clinic to identify β-amyloid (Aβ) aggregates (AMYViD ([^{18}F]AV-45), Neuraceq, Vizamyl, and [^{11}C]Pittsburgh Compound B ([^{11}C]PiB), Figure 1).[3−5] While the approved tracers have high cortical uptake in AD patients and have demonstrated value in detecting Aβ aggregates present in AD, they all suffer from subcortical nonspecific white matter binding.[6] Novel radioligands for AD that move beyond the current radiopharmaceuticals based on histological dyes for Aβ aggregates could help to further understand the pathogenesis of AD. To that end, we have worked on developing radioligands based on the metal hypothesis of AD, where the ideal ligand has a high affinity to metal-Aβ aggregates.

There is a growing body of evidence for the metal hypothesis of Alzheimer's disease. Metal ions, notably Cu, Zn, and Fe species, are present in aberrantly high concentrations in Aβ aggregates.[7] These ions are thought to contribute to Aβ

Received: October 9, 2014
Accepted: November 9, 2014
Published: November 9, 2014

DOI: 10.1021/ml500413d
ACS Med. Chem. Lett. 2015, 6, 112−116

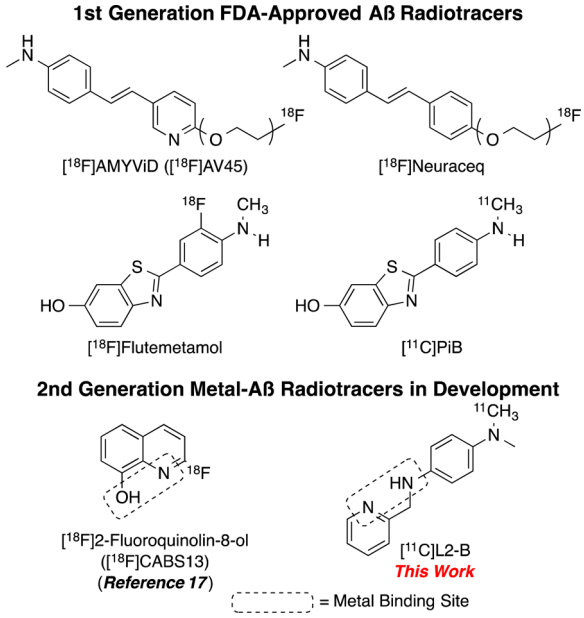

Figure 1. [^{11}C]L2-b and [^{18}F]CABS13.

aggregation,[8,9] and the resulting redox-active cationic metal species. The metal ions in Aβ are believed to mediate the formation of neurotoxic reactive oxygen species (ROS).[10−12] In particular, the Cu^{2+} ion binds to Aβ with high affinity[13] and has been shown to potentiate Aβ neurotoxicity.[11,14,15] To study metal ion mediated aggregation and disaggregation of Aβ *in vitro*, Lim et al. developed the compound N^1,N^1-dimethyl-N^4-(pyridin-2-ylmethyl) benzene-1,4-diamine (L2-b).[16] The molecule was designed as a bifunctional ligand, having affinity to Aβ and the ability to chelate metals (Figure 1). This was accomplished by modifying the stilbene scaffold, which was used previously as the starting point for AMYVid, to include a *N*,*N* bidentate chelating moiety.

In the evaluation of L2-b as a bifunctional ligand, it was demonstrated to bind metal-Aβ, to selectively chelate Cu^{2+} at physiological pH, and it was predicted to be blood−brain barrier (BBB) permeable.[16] Previously, Vasdev et al. reported a radioligand, [^{18}F]CABS13 (Figure 1),[17] derived from the 8-hydroxyquinoline scaffold shared by chelators clioquinol (CQ) and hydroxyquinoline (PBT2), which have shown some success in halting cognitive deterioration in clinical studies of familial AD.[18,19] Vasdev's preliminary preclinical work with [^{18}F]-CABS13 in a double transgenic mouse model of AD demonstrated it had promise as an imaging agent for AD. However, in ^{1}H−^{15}N TROSY-HSQC NMR experiments, L2-b was found to have a more pronounced effect on chemical shifts with monomeric Aβ than 8-hydroxyquinoline during titration,[16] suggesting L2-b has greater interaction and could outperform compounds based on 8-hydroxyquinoline.

These properties and the straightforward means to incorporate carbon-11, via methylation of the terminal aniline, made L2-b a good candidate to develop into a PET probe to examine the metal hypothesis of AD. Considering the longer half-life of fluorine-18 (109.77 min vs 20.33 min for carbon-11), L-2b was also interesting as the pyridine ring made it amenable to nucleophilic-aromatic substitution with fluorine-18. In this work, we describe the concise synthesis and preliminary preclinical evaluation of [^{11}C]L2-b and its fluorinated analogue [^{18}F]FL2-b. We hypothesize that PET probes targeting metal-Aβ aggregates will provide a way to understand the role metal ions play in the pathogenesis of AD and to identify Aβ aggregates with reduced nonspecific binding compared to existing radioligands.

To access radiotracers, it is necessary to synthesize both the precursors to be radiolabeled, and the corresponding unlabeled reference standards to confirm identity of the radiolabeled products by HPLC. The L2-b reference standard (**1**) was prepared in accordance with literature precedent through a reductive amination and was obtained in 47% yield (Scheme 1).[16] The FL2-b reference standard (**2**) was produced in a similar reaction using the 6-fluoro analogue of the corresponding aldehyde. This reaction furnished enough material for our purposes, despite only proceeding in 4% yield. This low yield is attributed to competing side reactions (e.g., nucleophilic aromatic substitution). In addition, the chloro-substituted precursor (**3**) required for fluorine-18 labeling was prepared using the same procedure. This reaction proceeded in higher 66% yield, presumably because the chloro-substituted pyridine is less amenable to competing nucleophilic substitution than its fluoro-substituted counterpart.

Scheme 1. Synthesis of L2-b Reference Standard (1), [^{18}F]FL2-b Reference Standard (2), and FL2-b Precursor (3)[a]

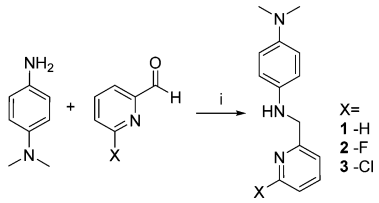

[a]Reagents and conditions: (i) $NaSO_4$, MeOH, r.t., 12 h; $NaBH_4$, MeOH, 0 °C; **1**, 47%, **2**, 4%, **3**, 66%.

The desmethyl precursor for [^{11}C]L2-b (**6**) was produced in a multistep synthesis (Scheme 2) beginning with the Boc protection of commercially available *N*-methyl-4-nitroaniline. The *p*-nitro group was reduced to primary amine (**4**).[20] This aniline was used in a reductive amination with 6-pyridine carboxyaldehyde to yield intermediate (**5**), which was converted to the precursor for [^{11}C]L2-b (**6**) by removal of the Boc group. As the aniline precursor to L2-b has two potential sites for methylation, both secondary amines, we wanted to ensure the radiolabeled product was the correct regioisomer (given the small amount of carbon-11 generated for a radiochemical synthesis, methylation of both sites on a single molecule is not expected). To alleviate our concern the alternate methylation product (**8**) was synthesized (Scheme 2) for later HPLC analysis of carbon-11 labeled products. Alternate methylation reference standard (**8**) was synthesized from (**5**) via a reductive amination with formaldehyde to install the methyl group. This resulting intermediate (**7**) was deprotected as before to produce the alternate methylation standard. The low synthetic yield for the route (~1% overall from (**5**)) produced a sufficient amount for our needs as an HPLC reference standard. An HPLC method was developed that could resolve the two potential methylation products (see Supporting Information). With all of the required reference standards and precursors in hand, our focus shifted to the radiochemical synthesis of [^{11}C]L2-b and its fluorine-18 analogue [^{18}F]FL2-b.

DOI: 10.1021/ml500413d
ACS Med. Chem. Lett. 2015, 6, 112−116

Scheme 2. Synthesis of [^{11}C]L2-b Precursor (6) and Alternate Methylation Reference Standard (8)[b]

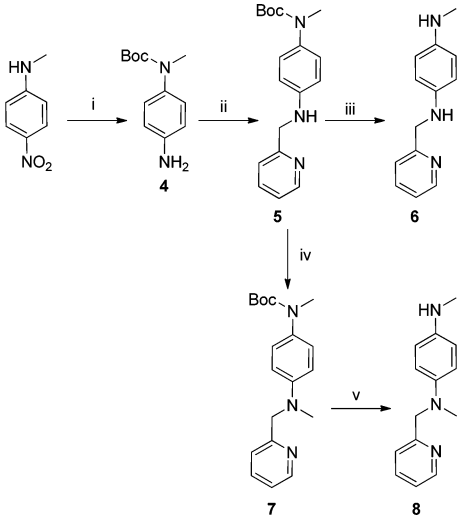

[b]Reagents and conditions: (i) Boc-anhydride, 4-DMAP, DCM, 12 h, 40 °C; Fe, NH_4Cl, MeOH, THF, 3 h, 70 °C, 74%; (ii) 4-pyridinecarboxyaldehyde, $NaSO_4$, MeOH, r.t. 12 h, 60%; (iii) TMSCl, MeOH, 2 4h, 0 °C, 90%; (iv) formaldehyde, MeOH; $NaBH_4$, MeOH, 0 °C, 2 h, 4.3%; (v) TMSCl, MeOH, 24 h, 0 °C, 60%.

The radiochemical synthesis of [^{11}C]L2-b followed literature techniques in common use in our laboratory.[21] Precursor (**6**) was dissolved in acetonitrile and deposited as a thin film in the steel HPLC loop of a TRACERlab FXc-pro carbon-11 synthesis module. [^{11}C]CO_2 (~3 Ci) was produced in a cyclotron via the ^{14}N(p,α)^{11}C nuclear reaction and delivered to the synthesis module where it was first reduced to [^{11}C]CH_4 by treating with hydrogen over a nickel catalyst at 350 °C. [^{11}C]CH_4 was then reacted with iodine at 750 °C to yield [^{11}C]CH_3I, which in turn was passed through a column of AgOTf at 200 °C to yield [^{11}C]MeOTf (~750 mCi, ~26% yield from [^{11}C]CO_2). [^{11}C]MeOTf was then passed through the loop for 5 min to produce [^{11}C]L2-b (**9**), which was purified by semipreparative HPLC. Subsequent reconstitution of the product fraction into ethanolic saline yielded doses of [^{11}C]L2-b [27 mCi, 3.6% nondecay corrected radiochemical yield based on [^{11}C]MeOTf, >95% radiochemical purity, 4550 Ci/mmol specific activity, n = 3] suitable for use in animal imaging studies. Both [^{18}F]FL2-b and [^{11}C]L2-b are susceptible to autoradiolytic decomposition; this necessitated the use of antioxidant stabilizer (ascorbic acid) in line with known literature techniques.[22] Additionally, HPLC purification proved difficult at low to neutral pH. This necessitated the use of a high-pH mobile phase and a column able to withstand a basic eluant (Phenomenex Gemini-NX). Reformulation into ethanolic saline or sterile water resulted in final doses with acceptable pH values (pH = 5.5) for evaluation in animal studies.

To produce FL2-b, precursor (**3**) was dissolved in DMSO and treated with [^{18}F]KF in the presence of 2.2.2-cryptand at 130 °C for 30 min (Scheme 3). The reaction was quenched with HPLC eluant, and the product was purified from the reaction mixture by semipreparative HPLC. The product fraction was reconstituted into ethanolic saline and collected as a dose of [^{18}F]FL2-b [2.49 mCi, 1.0% nondecay corrected radiochemical yield, >99% radiochemical purity, 970 Ci/mmol

Scheme 3. Radiochemical Synthesis of [^{11}C]L2-b (9) and [^{18}F]FL2-b (10)[c]

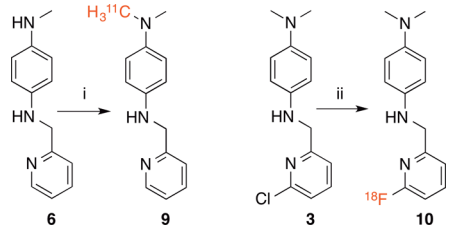

[c]Reagents and conditions: (i) [^{11}C]MeOTf, MeCN, 5 min, 3.6% RCY; (ii) [^{18}F]KF, 2.2.2 cryptand, DMF, 130 °C, 30 min, 1.0% RCY.

specific activity, n = 3] suitable for use in post-mortem tissue analysis.

With radiochemical synthesis methods developed, we conducted preliminary experiments to validate the probes as Aβ radioligands. The affinity of both probes for Aβ aggregates were assessed through experiments utilizing post-mortem human brain tissue (20 μm thick sections) from both AD positive patients and normal controls, visualized and quantitated by autoradiography (Figure 2). The K_d for[^{11}C]-

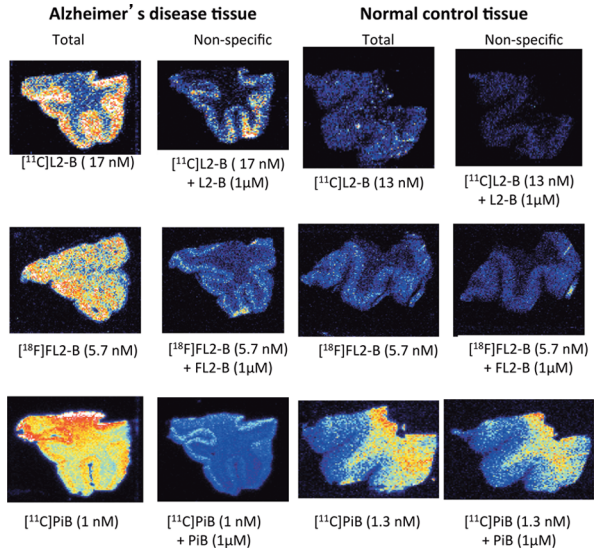

Figure 2. Post-mortem tissue binding autoradiography images.

L2-b and [^{18}F]FL2-b were found to be 3.5 and 9.4 nM, respectively, and associated B_{max} values were found to be 0.032 and 0.016 fmol/mm^2, respectively. The lower affinity of [^{18}F]FL2-b may be attributed to the electron withdrawing properties of fluorine from the *N*,*N* metal chelating center. Nonspecific binding was determined by washing tissue with 1 μM of the nonlabeled reference standard. In our experiments, neither L2-b nor FL2-b were found to exhibit retention in normal control tissue or high white matter uptake observed with PiB.

Displacement studies (n = 2) were performed with [^{11}C]L2-b radioligand in human brain tissue (Figure 3). AD tissue was pretreated with [^{11}C]L2-b, and then treated with 1 μM of nonlabeled AV-45, PiB, or L2-b reference standard. L2-b was found to readily displace itself (80% displaced), and PiB was also reasonably effective at displacing [^{11}C]L2-b (46%). AV-45 was found to only displace 5% of bound [^{11}C]L2-b. Considering its low-nanomolar affinity[23] and structural

DOI: 10.1021/ml500413d
ACS Med. Chem. Lett. 2015, 6, 112−116

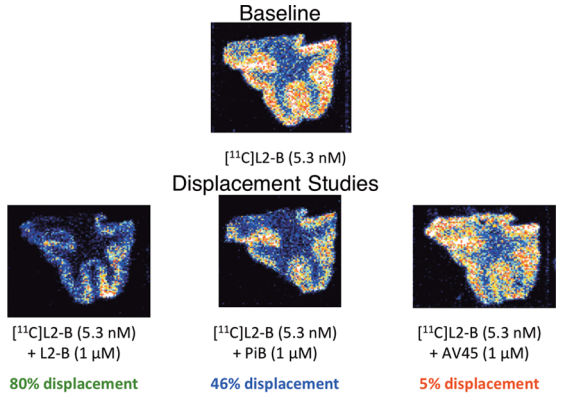

Figure 3. Displacement study images.

similarity, AV-45 would be expected to readily displace L2-b at such high concentration. This implies that AV-45 binds in a different location or manner than L2-b. In view of the amorphous nature of Aβ species, it is difficult to assert an exact binding pocket, but studies with Congo Red and Thioflavin T indicate π-bond rich, small molecules bind in grooves of β-sheets characteristic to Aβ fibrils.[24,25] AV-45 may fail to displace L2-b due to L2-b forming a ligand−metal-Aβ complex as proposed by Lim et al.,[16] and AV-45 lacks the metal-interaction capacity to disrupt the complex. PiB, while lacking the stilbene-like scaffold, could potentially displace L2-b from metal-Aβ at high concentrations as benzothiazole derivatives have been shown to act as ligands in metal complexes.[26,27] This suggests that L2-b has affinity for metal-Aβ.

The positive results from the tissue studies led to the examination of the imaging properties of [^{11}C]L2-b in nonhuman primates (Figure 4a). We decided to use [^{11}C]L2-b as it exhibited the lower K_d in our post-mortem binding study. The brain uptake and efflux of [^{11}C]L2-b was assessed *in vivo* with nonhuman primate microPET imaging (n = 2). Drawing straightforward region-of-interests (ROI) around the whole brain, cortex, and cerebellum, time-radioactivity curves were generated for each region (Figure 4b). In a healthy primate, brisk initial uptake (peak standardized uptake value (SUV) = 2.0 at 2.5 min) was observed throughout all brain regions, followed by rapid egress of the radiotracer from the brain. This was the expected finding for a healthy primate brain containing no amyloid burden. The data confirms that the scaffold is BBB permeable and, along with the high signal-to-noise ratio in the post-mortem tissue analysis, demonstrates that L2-b and molecules based on the scaffold are attractive candidate radiotracers for using PET to elucidate the complex mechanisms underlying the metallobiology of AD.

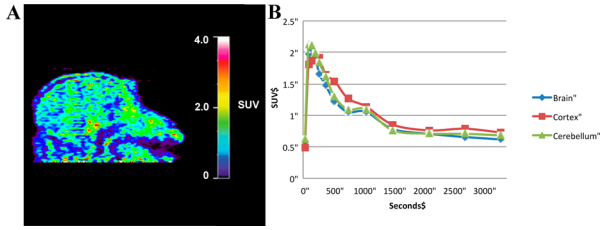

Figure 4. Summed (0−60 min following i.v. injection of the radiotracer) nonhuman primate microPET images (A) and corresponding time−radioactivity curves (B).

This proof-of-concept and preliminary preclinical examination demonstrates that L2-b is a scaffold of interest for quantifying metal-Aβ species *in vivo*. Considering imaging issues with earlier generation Aβ probes and the mounting evidence for the metal hypothesis of Alzheimer's disease, further investigation into and with metal-Aβ radioligands is warranted.

■ ASSOCIATED CONTENT

Ⓢ Supporting Information

Full experimental details for all compounds synthesized; copies of NMR, MS, and HPLC spectra/chromatograms for standards and precursors; procedures for radiochemical syntheses and quality control; protocols for microPET animal imaging studies, autoradiography, and immunohistochemistry. This material is available free of charge via the Internet at http://pubs.acs.org.

■ AUTHOR INFORMATION

Corresponding Author

*E-mail: pjhscott@umich.edu. Tel: +1 (734) 615-1756. Fax: +1 (734) 615-2557.

Author Contributions

#These authors contributed equally to this work. The manuscript was written through contributions of all authors. All authors have given approval to the final version of the manuscript.

Funding

Financial support of this work from the National Institute of Biomedical Imaging and Bioengineering, part of the National Institutes of Health (under Award Number T32-EB005172) is gratefully acknowledged. The content of this article is solely the responsibility of the authors and does not necessarily represent the official views of the National Institutes of Health. Additional funding for this research from the Alzheimer's Association (under award number NIRP-14-305669), the University of Michigan Office of the Vice President for Research, and the University of Michigan Undergraduate Research Opportunity Program (UROP) is gratefully acknowledged. The Michigan Alzheimer's Disease Center is funded by the National Institute of Aging (under Award Number P50-AG08671) as well as a gift from an anonymous donor.

Notes

The authors declare no competing financial interest.

Biography

Peter J. H. Scott received his Ph.D. in Organic Chemistry from Durham University in the United Kingdom. Following postdoctoral training at SUNY Buffalo and the University of Michigan, he returned to the University of Michigan and is currently Assistant Professor of Radiology, Director of the PET Center, and a member of the Interdepartmental Program in Medicinal Chemistry. Scott's group designs new radiotracers for PET imaging of CNS disorders such as Alzheimer's disease with the goals of improving our understanding of disease mechanisms and, ultimately, using them as companion diagnostics to support therapeutic development. His group also develops new methods for radiolabeling of bioactive molecules, and his laboratory is funded by the U.S. Department of Energy, the National Institute of Biomedical Imaging and Bioengineering, and the Alzheimer's Association.

DOI: 10.1021/ml500413d
ACS Med. Chem. Lett. 2015, 6, 112−116

■ ACKNOWLEDGMENTS

The authors thank the Michigan Alzheimer's Disease Center (MADC) Brain Bank for selecting and providing brain samples.

■ ABBREVIATIONS

AD, Alzheimer's disease; Aβ, beta-amyloid; BBB, blood−brain barrier; Boc, *tert*-butyloxycarbonyl; CNS, central nervous system; DMAP, 4-dimethylaminopyridine; DMSO, dimethyl sulfoxide; DCM, dicholormethane; HPLC, high-performance liquid chromatorgraphy; PBT2, hydroxyquinoline; PET, positron emission tomography; PiB, Pittsburgh Compound-B; ROI, region-of-interest; THF, tetrahydrofuran; TMSCl, trimethylsilyl chloride; UV, ultraviolet

■ REFERENCES

(1) Plassman, B. L.; Langa, K. M.; Fisher, G. G.; Heeringa, S. G.; Weir, D. R.; Ofstedal, M. B.; Burke, J. R.; Hurd, M. D.; Potter, G. G.; Rodgers, W. L.; Steffens, D. C.; Willis, R. J.; Wallace, R. B. Prevalence of Dementia in the United States: The Aging, Demographics, and Memory Study. *Neuroepidemiology* **2007**, *29*, 125−132.

(2) Duthey, B.Update on 2004 Background Paper Alzheimer Disease and Other Demntias. *Priority Medicines for Europe and the World; A Public Health Approach to Innovation*; WHO: Geneva, Switzerland, 2013.

(3) Klunk, W. E.; Engler, H.; Nordberg, A.; Wang, Y.; Blomqvist, G.; Holt, D. P.; Bergström, M.; Savitcheva, I.; Huang, G.-F.; Estrada, S.; Ausén, B.; Debnath, M. L.; Barletta, J.; Price, J. C.; Sandell, J.; Lopresti, B. J.; Wall, A.; Koivisto, P.; Antoni, G.; Mathis, C. A.; Långström, B. Imaging brain amyloid in Alzheimer's disease with Pittsburgh Compound-B. *Ann. Neurol.* **2004**, *55*, 306−319.

(4) Wong, D. F.; Rosenberg, P. B.; Zhou, Y.; Kumar, A.; Raymont, V.; Ravert, H. T.; Dannals, R. F.; Nandi, A.; Brašić, J. R.; Ye, W.; Hilton, J.; Lyketsos, C.; Kung, H. F.; Joshi, A. D.; Skovronsky, D. M.; Pontecorvo, M. J. In Vivo Imaging of Amyloid Deposition in Alzheimer Disease Using the Radioligand 18F-AV-45 (Flobetapir F 18). *J. Nucl. Med.* **2010**, *51*, 913−920.

(5) Chételat, G.; La Joie, R.; Villain, N.; Perrotin, A.; de La Sayette, V.; Eustache, F.; Vandenberghe, R. Amyloid Imaging in Cognitively Normal Individuals, at-Risk Populations and Preclinical Alzheimer's Disease. *NeuroImage: Clin.* **2013**, *2*, 356−365.

(6) Rowe, C. C.; Villemagne, V. L. Brain Amyloid Imaging. *J. Nucl. Med. Technol.* **2013**, *41*, 11−18.

(7) Lovell, M. A.; Robertson, J. D.; Teesdale, W. J.; Campbell, J. L.; Markesbery, W. R. Copper, Iron and Zinc in Alzheimer's Disease Senile Plaques. *J. Neurol. Sci.* **1998**, *158*, 47−52.

(8) Faller, P.; Hureau, C.; Berthoumieu, O. Role of Metal Ions in the Self-Assembly of the Alzheimer's Amyloid-β Peptide. *Inorg. Chem.* **2013**, *52*, 12193−12206.

(9) Hane, F.; Leonenko, Z. Effect of Metals on Kinetic Pathways of Amyloid-β Aggregation. *Biomolecules* **2014**, *4*, 101−116.

(10) Hewitt, N.; Rauk, A. Mechanism of Hydrogen Peroxide Production by Copper-Bound Amyloid Beta Peptide: A Theoretical Study. *J. Phys. Chem. B* **2009**, *113*, 1202−1209.

(11) Sharma, A. K.; Pavlova, S. T.; Kim, J.; Kim, J.; Mirica, L. M. The Effect of Cu^{2+} and Zn^{2+} on the Aβ42 Peptide Aggregation and Cellular Toxicity. *Metallomics* **2013**, *5*, 1529−1536.

(12) Markesbery, W. R. Oxidative Stress Hypothesis in Alzheimer's Disease. *Free Radic. Biol. Med.* **1997**, *23*, 134−147.

(13) Hatcher, L. Q.; Hong, L.; Bush, W. D.; Carducci, T.; Simon, J. D. Quantification of the Binding Constant of Copper(II) to the Amyloid-Beta Peptide. *J. Phys. Chem. B* **2008**, *112*, 8160−8164.

(14) Huang, X.; Cuajungco, M. P.; Atwood, C. S.; Hartshorn, M. A.; Tyndall, J. D. A.; Hanson, G. R.; Stokes, K. C.; Leopold, M.; Multhaup, G.; Goldstein, L. E.; Scarpa, R. C.; Saunders, A. J.; Lim, J.; Moir, R. D.; Glabe, C.; Bowden, E. F.; Masters, C. L.; Fairlie, D. P.; Tanzi, R. E.; Bush, A. I. Cu(II) Potentiation of Alzheimer Aβ neurotoxicity: Correlation with Cell-Free Hydrogen Peroxide Production and Metal Reduction. *J. Biol. Chem.* **1999**, *274*, 37111−37116.

(15) Tougu, V.; Tiiman, A.; Palumaa, P. Interactions of Zn(II) and Cu(II) Ions with Alzheimer's Amyloid-Beta Peptide. Metal Ion Binding, Contribution to Fibrillization and Toxicity. *Metallomics* **2011**, *3*, 250−261.

(16) Choi, J.-S.; Braymer, J. J.; Nanga, R. P. R.; Ramamoorthy, A.; Lim, M. H. Design of Small Molecules That Target Metal-Aβ Species and Regulate Metal-Induced Aβ Aggregation and Neurotoxicity. *Proc. Natl. Acad. Sci. U.S.A.* **2010**, *107*, 21990−21995.

(17) Vasdev, N.; Cao, P.; van Oosten, E. M.; Wilson, A. A.; Houle, S.; Hao, G.; Sun, X.; Slavine, N.; Alhasan, M.; Antich, P. P.; Bonte, F. J.; Kulkarni, P. Synthesis and PET Imaging Studies of [^{18}F]2-Fluoroquinolin-8-ol ([^{18}F]CABS13) in Transgenic Mouse Models of Alzheimer's Disease. *Med. Chem. Commun.* **2012**, *3*, 1228−1230.

(18) Duce, J. A.; Bush, A. I. Biological Metals and Alzheimer's Disease: Implications for Therapeutics and Diagnostics. *Prog. Neurobiol.* **2010**, *92*, 1−18.

(19) Ibach, B.; Haen, E.; Marienhagen, J.; Hajak, G. Clioquinol Treatment in Familiar Early Onset of Alzheimer's Disease. *Pharmacopsychiatry* **2005**, *38*, 178−179.

(20) Yan, S.; Wang, L.; Frye, L. L.; Chen, W.; Loury, D. J. Purinone Compounds as Kinase Inhibitors. WO Patent WO2013116382 A1, 2013.

(21) Shao, X.; Hoareau, R.; Runkle, A. C.; Tluczek, L. J. M.; Hockley, B. G.; Henderson, B. D.; Scott, P. J. H. Highlighting the Versatility of the Tracerlab Synthesis Modules. Part 2: Fully Automated Production of [^{11}C]-Labeled Radiopharmaceuticals Using a Tracerlab $FX_{C\text{-}Pro}$. *J. Labelled Comp. Radiopharm.* **2011**, *54*, 819−838.

(22) Scott, P. J. H.; Hockley, B. G.; Kung, H. F.; Manchanda, R.; Zhang, W.; Kilbourn, M. R. Studies into Radiolytic Decomposition of Fluorine-18 Labeled Radiopharmaceuticals for Positron Emission Tomography. *Appl. Radiat. Isot.* **2009**, *67*, 88−94.

(23) Choi, S. R.; Golding, G.; Zhuang, Z.; Zhang, W.; Lim, N.; Hefti, F.; Benedum, T. E.; Kilbourn, M. R.; Skovronsky, D.; Kung, H. F. Preclinical Properties of ^{18}F-AV-45: A PET Agent for Aβ Plaques in the Brain. *J. Nucl. Med.* **2009**, *50*, 1887−1894.

(24) Wu, C.; Scott, J.; Shea, J.-E. Binding of Congo Red to Amyloid Protofibrils of the Alzheimer Aβ9-40 Peptide Probed by Molecular Dynamics Simulations. *Biophys. J.* **2012**, *103*, 550−557.

(25) Khurana, R.; Coleman, C.; Ionescu-Zanetti, C.; Carter, S. A.; Krishna, V.; Grover, R. K.; Roy, R.; Singh, S. Mechanism of Thioflavin T Binding to Amyloid Fibrils. *J. Struct. Biol.* **2005**, *151*, 229−238.

(26) Huynh, H. V.; Meier, N.; Pape, T.; Hahn, F. E. Benzothiazolin-2-ylidene Complexes of Iridium(I). *Organometallics* **2006**, *25*, 3012−3018.

(27) Stey, T.; Pfeiffer, M.; Henn, J.; Pandey, S. K.; Stalke, D. Di(benzothiazol-2-yl)phosphanide as a Janus-Head Ligand to Caesium. *Chem.—Eur. J.* **2007**, *13*, 3636−3642.

■ NOTE ADDED AFTER ASAP PUBLICATION

This paper was published ASAP on November 11, 2014, with incorrect versions of Scheme 3 and the Supporting Information. These items were corrected in the version published ASAP on December 1, 2014.

DOI: 10.1021/ml500413d
ACS Med. Chem. Lett. 2015, 6, 112−116